Journal of Inflammation Research

Dovepress
Taylor & Francis Group

Open Access Full Text Article

ORIGINAL RESEARCH

Single-Cell RNA-Seq Uncovers Cellular Heterogeneity from Deep Fascia in Necrotizing Fasciitis Patients

Tao Wang[1,*], Liping Zhang[2,*], Wei Chen[3], Yubin Long[3], Yingze Zhang[3–6], Ling Wang[3], Zhiyong Hou[3–6]

[1]Department of Lower Limb Trauma, Beijing Jishuitan Hospital, Guizhou Hospital, Guiyang, Guizhou, People's Republic of China; [2]Department of Physiology, Hebei Medical University, Shijiazhuang, Hebei, People's Republic of China; [3]Department of Orthopaedic Surgery, Third Hospital of Hebei Medical University, Shijiazhuang, Hebei, People's Republic of China; [4]Engineering Research Center of Orthopedic Minimally Invasive Intelligent Equipment, Ministry of Education, Shanghai, People's Republic of China; [5]Key Laboratory of Biomechanics of Hebei Province, Shijiazhuang, Hebei, People's Republic of China; [6]NHC Key Laboratory of Intelligent Orthopaedic Equipment, Shijiazhuang, Hebei, People's Republic of China

*These authors contributed equally to this work

Correspondence: Zhiyong Hou, Department of Orthopaedic Surgery, Third Hospital of Hebei Medical University, Shijiazhuang, Hebei, P.R. China. No. 139 Road Ziqiang, Shijiazhuang, Hebei, People's Republic of China, Email drzyhou@gmail.com

Purpose: Necrotizing fasciitis (NF) is a scarce but potentially life-threatening infection. However, no research has reported the cellular heterogeneity in patients with NF. We aim to investigate the change of cells from deep fascia in response to NF by single-cell RNA-seq.

Methods: Fascia samples from NF patients (NF group, NG, n = 3) and volunteer (control group, CG, n = 4) were obtained and we utilized scRNA-seq to observe the variation of cells and differentially expressed genes. Then, multiplex staining and multispectral imaging and immunohistochemistry were used to be further verified.

Results: Our findings showed that three fibroblast subclusters (antigen-presenting Fib, mesenchymal Fib, and myoFib) and three macrophage subclusters ($SPP1^+$ Mac0, $IL1B^+$ Mac1, and $SPP1^+$M2) were found to have increased proportions with distinct roles in NF patients. The balance of M1/M2 polarization may be the key therapeutic target to determine the outcome of NF. Furthermore, the levels of SAA1, PTX3, S100 family, MARCO, and STAB1 were up-regulated in different subclusters with anti-infection roles against NF, which were proven by immunohistochemistry. These proteins may act as a biomarker or even as a candidate therapy for NF.

Conclusion: Our findings revealed the potential anti-infection role of deep fascia during the procession of NF, helping us understand the immunologic function of fascia and provide novel insights for its therapeutic strategies for NF.

Keywords: necrotizing fasciitis, deep fascia, single-cell RNA-seq, M1/M2 polarization, fibroblast

Introduction

Necrotizing fasciitis (NF) is an uncommon but serious and promptly progressive infection characterized by necrosis of subcutaneous tissue and fascia,[1,2] influencing from 0.4 per 100,000 individuals to 15.5 cases per 100,000 people, according to previous studies.[2,3] NF was classified as *polymicrobial* (type-I), or *monomicrobial* (type-II),[4,5] and type-III was reported to be caused by *Vibrio spp*. based on recent studies.[3,6,7] Type-I has been considered to be more prevalent than type-II,[8] while the latest studies have reported monomicrobial NF with a higher incidence.[9,10] Rapid debridement and broad-spectrum antibiotics are the gold standards in the treatment of NF, which may cause morbidities, such as deformity, limb loss, systemic toxicity, or even organ failure.[11–13] Its mortality is as high as 30% and even reaches 70% once an incorrect or delayed diagnosis is made.[14,15]

It is challenging for clinicians to separate NF from non-necrotizing infections at an early stage due to the paucity of early pathognomonic signs. Conceptually, recognizing its risk factors, identifying its biomarkers, and gaining an in-depth understanding of its potential mechanisms can accelerate and improve the management of this devastating infection.

Received: 8 October 2024
Accepted: 12 January 2025
Published: 22 January 2025

Wong[16] invented the Necrotizing Fasciitis score to discern NF from other soft-tissue infections. Zhu[17] identified 126 genes of M1 and 116 genes of M28 by insertion-site sequencing. Thänert[18] used 16S rRNA sequencing and RNA sequencing to identify the molecular mechanisms underlying the pathophysiology of NF. These findings have provided possible targets for future therapeutic strategies.

Recent studies have mainly focused on the microbial etiologies of NF, yet studies solving pathological mechanisms and exploring dynamic variations of cells in NF are lacking. Additionally, studies on the host response to NF are absent and the role of deep fascia in NF remains completely unknown. We assume the variations of cellular subtypes of fascia against this life-threatening infection. To verify these hypotheses, we are the first to use single-cell RNA sequencing (scRNA-seq) to observe the variation of cells, and cell-to-cell interactions of the fascia in NF patients. We provide bio-information to help us recognize the fascia and uncover its functions in the process of NF, which may provide novel insights into future therapeutic strategies.

Methods

Patient Recruitment and Ethics

Fascia samples were obtained from patients with NF as the NF group (NG, n = 3) and from donors as the control group (CG, n = 4) in our hospital (Figure 1a). Fascia samples from patients with NF were obtained as part of a routine surgical procedure, and informed consent was obtained from NF patients. Donors were recruited from July 2022 to October 2022 based on the following inclusion/exclusion criteria. Inclusion criteria: (1) adult patients (>18 years old); (2) sudden death due to car accident. Exclusion criteria: (1) the sampling part has a history of surgery or infection; (2) with a history of immune system diseases, such as systemic lupus erythematosus; (3) chronic diseases, such as diabetes, heart disease, or kidney disease. Fascia samples from donors were obtained with consent from the family. Characteristics of patients is shown in Table 1. Our study was approved by the Third Hospital of Hebei Medical University Ethics Committee (No. S2020-024-1) in compliance with the declaration of Helsinki.

Sample Preparation and Tissue Dissociation

We used 1× PBS to purge blood spots and adipose tissue from fascia samples and cut them into 0.5 mm^2 fragments. Next, we used dissociation solution (0.35% collagenase IV5, 2 mg/mL papain, 120 units/mL DNase I) to dissociate them into single cells in a 37°C water bath with shaking at 100 rpm for 20 minutes. Decomposition was stopped by pipetting 5–10 times with a Pasteur pipette in 1× PBS containing 10% fetal bovine serum (FBS, V/V). The concentration of single-cell suspensions was adjusted to 700–1200 cells/μL and overall cell viability was required to be more than 85%.

Chromium 10x Genomics Library and Sequencing

Based on the instructions, single-cell suspensions were put in 10x Chromium to capture 8000 single cells. The processes for cDNA amplification and library creation were carried out according to the conventional procedure. LC-Bio Technology Co., Ltd. (Hangzhou, China) sequenced libraries using an Illumina NovaSeq 6000 sequencing system (paired-end multiplexing run, 150 bp) at a minimum depth of 20,000 reads per cell (Figure 1a).

Single-Cell RNA-Seq Data Processing and Data Visualization

We used Cell Ranger pipeline (version 6.1.1) to demultiplex samples, process barcodes, and count single-cell 3' genes, and scRNA-seq data were aligned to the GRCh38 reference genome in Ensembl. We used 10X Genomics Chromium Single Cell 3' Solution to capture 54936 single cells from our patients, which passed the following quality control threshold (Figure 1a): (1) Genes expressed in multiple cells, (2) each cell with more than 500 expressed genes and (3) <25% of gene expression from mitochondrial DNA. We used DoubletFinder to remove doubles.

Dimensionality Reduction and Annotation of Major Cell Types

We utilized Seurat to reduce the dimensionality. The number of unique molecular identifiers, percentage of mitochondrial genes, and genes were scaled to unit variance. Principal component analysis (PCA) was performed. Clusters were then identified using tSNE. Cell identity was assigned using known markers.

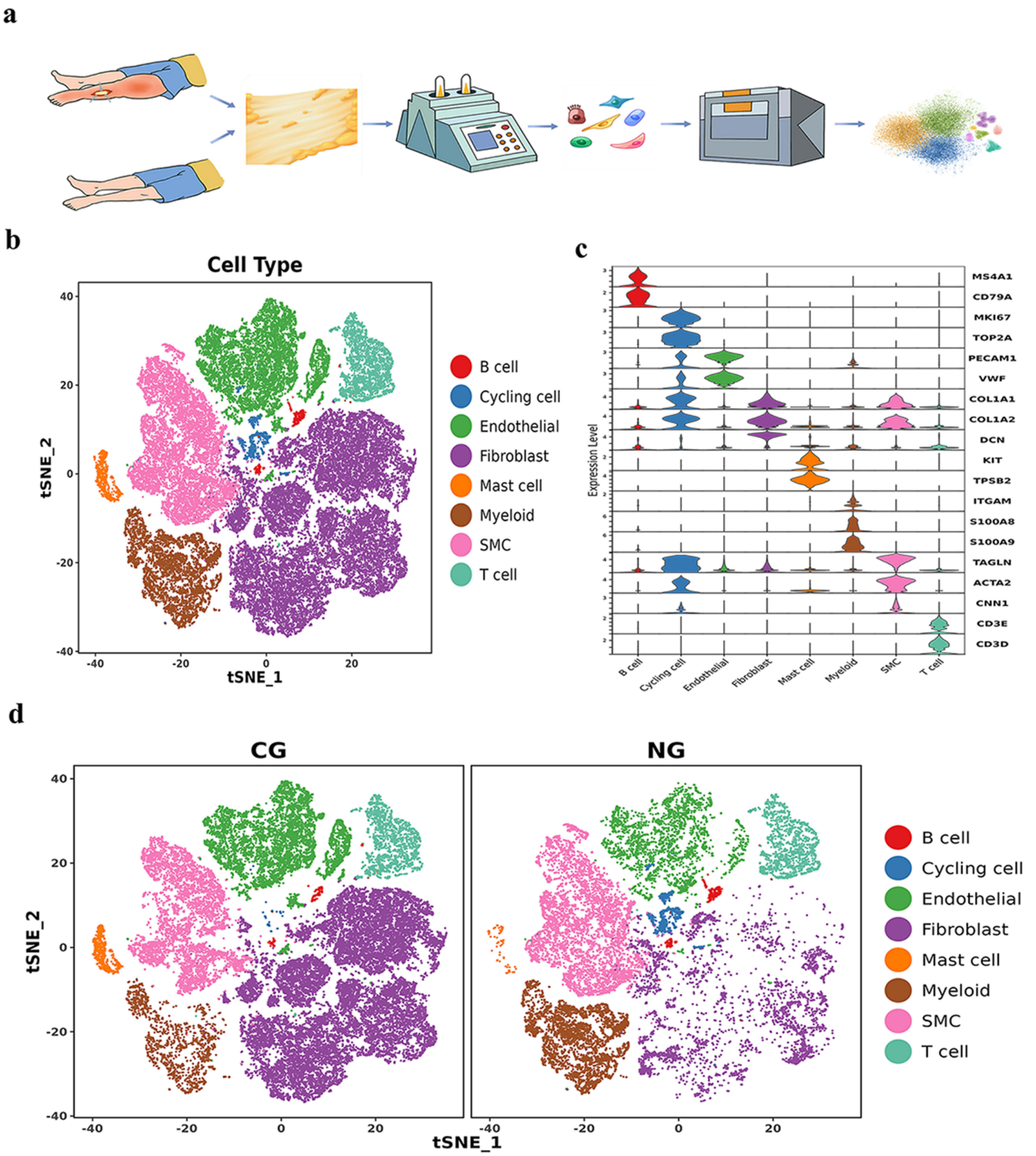

Figure 1 Clustering and classification of the cellular landscape of deep fascia tissue. (**a**). Overview of the experimental workflow. (**b**). tSNE visualization of cell cluster from deep fascia tissue. (**c**). Violin plots showing marker genes across cell clusters. (**d**). tSNE visualization of cell cluster from deep fascia tissue in NG and CG.
Abbreviations: scRNA-seq, single-cell RNA sequencing; NG, necrotizing fasciitis group; CG, control group.

Detection of Differentially Expressed Genes and Pathway Analysis

We applied the default parameters via the FindMarkers function in Seurat to compare DEGs of the same cell types between two groups, which were categorized by average log2 (fold change) after being processed with a minimum log2 (fold change) of 0.26 and a maximum adjusted p value of 0.01. We used Gene Ontology (GO) terms and Kyoto Encyclopedia of Genes and Genomes (KEGG) pathways to create the gene sets.

https://doi.org/10.2147/JIR.S496650

Table 1 Characteristics of Patients in Two Groups

No of Patient	Age(Years)	Sex	Diagnosis	Group	Sample Source
1	56	Male	Tibiofibular fracture	NG	Inside of middle shank
2	29	Male	Tibiofibular fracture	NG	Inside of middle shank
3	31	Male	Tibiofibular fracture	NG	Inside of middle shank
4	70	Male	Donator	CG	Inside of middle shank
5	45	Male	Donator	CG	Inside of middle shank
6	41	Male	Donator	CG	Inside of middle shank
7	51	Male	Donator	CG	Inside of middle shank

Abbreviations: NG, necrotizing fasciitis group; CG, control group.

Cell-Cell Interaction Analysis

We utilized CellPhoneDB (v3) to observe cell–cell interplay by ligand–receptor interactions. The normalized counts of cells in the two groups were independently downloaded and used as input for the CellPhoneDB method.

Multiplex Staining and Multispectral Imaging

We used multiplex staining and multispectral imaging to identify cell subsets of fascia by a PANO 5-plex IHC kit (cat 0004100100) (Panovue, Beijing, China). We applied SMA, CD31, CD14, CD3, and CD19 sequentially incubated with a secondary antibody conjugated to horseradish peroxidase and a tyramide signal amplification reagent. DAPI was labeled the location of each nucleus. We used Mantra System (PerkinElmer, Waltham, Massachusetts, US) to gain high-quality images with the fluorescence spectra at 20-nm wavelength intervals from 420 to 720 nm with identical exposure times.

Immunohistochemistry

Fascia tissues were fixed with 4% PFA overnight and prepared into paraffin-embedded sections and then were sliced into 4-μm-thick sections for immunohistochemistry (IHC) staining. Sections were incubated at 4°C overnight with the primary antibody. Then, anti-Fibronectin (Cat.#: 15,613-1-AP, Proteintech, China), anti-MARCO (Cat.#: CSB-PA880072ESR2HU, CUSABIO, China), anti-S100A9 (Cat.#: 26,991-1-AP, Proteintech, China), anti-S100A8 (Cat.#: R1706-20, Huabio, China), anti-Serum Amyloid A (Cat.#: 381812, ZEN BIO, China), anti-Stabilin-1 (Cat.#: 20,663-1-AP, Proteintech, China), anti-S100A12 (Cat.#: DF7277, Affinity, China), anti-Ptx3 (Cat.#: ER64704, Huabio, China) were diluted at 1/200. A streptavidin biotin complex kit (Cat.#: PV-9000, ZSGB-BIO, China) was used for subsequent steps. The localization of peroxidase was determined using a DAB kit (ZLI9018, ZSGB-BIO), and tissue sections were determined using digital imaging at 100× magnification.

Results

The Landscape of All Kinds of Cells in CG and NG

Ultimately, we gained 54936 cells by single-cell transcriptomes in two groups, consisting of 35851 cells in the CG and 19085 cells in the NG, following data preprocessing and quality control. We identified eight clusters, including B cells, cycling cells, endothelial cells, fibroblasts, mast cells, myeloid cells, smooth muscle cells, and T cells (Figure 1b-d). Figure 2a indicated the percentages of each cluster in each patients, and higher proportions of B cells, cycling cells, myeloid cells, SMC, and T cells, while lower proportions of endothelial cells, fibroblasts, and mast cells were found in the NG (Figure 2b and Table 2).

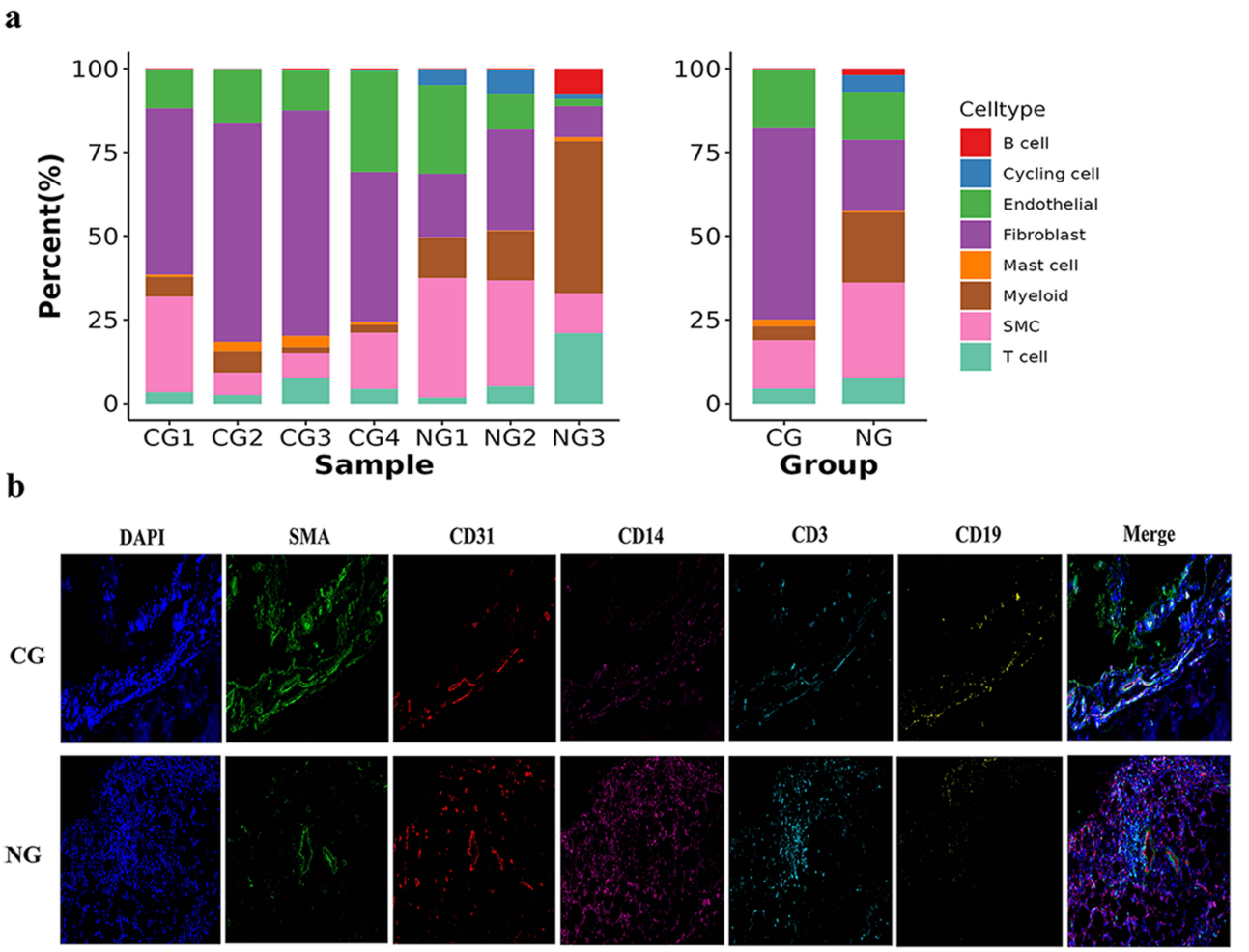

Figure 2 Percentage of cell cluster in two groups. (**a**). Bar plots showing the relative percentage of cell cluster for each sample as well as in two groups (NG and CG); (**b**). Multiplex staining and multispectral imaging showing fibroblasts and immune cell infiltration, including T cells and myeloid cells in NG compared with CG. *green (α-SMA): fibroblast; red (CD31): endothelial cells; pink (CD14): myeloid cells; blue (CD3): T cell; yellow (CD19): B cell.
Abbreviations: NG, necrotizing fasciitis group; CG, control group.

Fibroblast Subsets in the Two Groups

We identified five subtypes of fibroblasts (Fib): antigen-presenting Fib, inflammatory Fib, matrix Fib, mesenchymal Fib, and myoFib[19] (Figure 3a-c). Then, we found higher proportions of antigen-presenting Fib, mesenchymal Fib, and myoFib as well as a lower proportion of the matrix Fib subtype in the NG (Figure 3d and Table 2).

Next, we compared the top 10 DEGs of higher proportions of fibroblasts in the NG. Notably, we found that *TIMP1, BGN, CCL19, CHI3L1, IGHA1* and *IGKC* were up-regulated in antigen-presenting Fib (Figure 4a). The GO term showed that this subpopulation was associated with "neutrophil chemotaxis", "inflammatory response", "lymphocyte chemotaxis", and "defense response to bacterium" (Supplementary Figure 1). KEGG analysis indicated that the PI3K-Akt, NF-kappa B, HIF-1, and IL-17 signaling pathway may be involved in regulating NF (Supplementary Figure 2). In addition, *BGN, TNC, CHI3L1, CHI3L2, COL3A1, PTX3, SAA1, SAA2, SERPINE2*, and *STEAP4* were up-regulated in mesenchymal Fib. Then, we used IHC staining to verify the expression of PTX3 and SAA1 in two groups (Figure 4b). The GO term implied that this subpopulation was involved in "inflammatory response", "positive regulation of interleukin-8 production", and "response to tumor necrosis factor" (Supplementary Figure 1). KEGG pathway showed that the PI3K-Akt and Relaxin signaling pathway may be involved in regulating NF (Supplementary Figure 2). Furthermore, *TIMP1, CCL19, COL1A1, COL3A1, COL4A2, COL4A1, SAA1, STEAP4*, and *SPARC* were up-regulated in myoFib (Figure 4a). The GO term indicated that this subpopulation

Table 2 Proportion of All Cell Clusters or Subclusters in Two Groups

Clusters	CG	NG	P value
B cell	0.32%	1.97%	<0.0001
Cycling cell	0.13%	5.01%	<0.0001
Endothelial	17.36%	14.25%	<0.0001
Fibroblast	57.13%	21.30%	<0.0001
Mast cell	2.05%	0.42%	<0.0001
Myeloid	4.11%	20.96%	<0.0001
SMC	14.45%	28.42%	<0.0001
T cell	4.46%	7.67%	<0.0001
Fibroblast subclusters			
Antigen-presenting Fib	0.77%	1.97%	<0.0001
Inflammatory Fib	26.40%	24.99%	0.061
Matrix Fib	48.54%	29.56%	<0.0001
Mesenchymal Fib	19.50%	25.55%	<0.0001
MyoFib	4.79%	17.93%	<0.0001
Myeloid cell subclusters			
SPP1+ M0	1.63%	6.03%	<0.0001
IL1B+ M1	15.81%	27.78%	<0.0001
C1QA+ M2	46.74%	36.20%	<0.0001
IFN-act M2	1.63%	0.85%	0.013
SPP1+ M2	0.75%	6.75%	<0.0001
Monocyte	2.71%	13.93%	<0.0001
cDC1	1.63%	1.08%	0.099
cDC2	18.05%	3.48%	<0.0001
Other	11.06%	3.93%	<0.0001
T cell subclusters			
Cytotoxic CD8 T	25.94%	15.98%	<0.0001
GZMK+ CD4 Teff	50.75%	61.41%	<0.0001
GZMK+ CD8 Teff	9.31%	7.58%	0.086
ILC3	3.06%	3.07%	0.986
NK	2.13%	1.91%	0.677
NKT	7.75%	2.87%	<0.0001
Other	1.06%	7.17%	<0.0001

Notes: We showed the percentage in two groups and the P values were calculated by the chi-square test in raw data.
Abbreviations: NG, necrotizing fasciitis group; CG, control group.

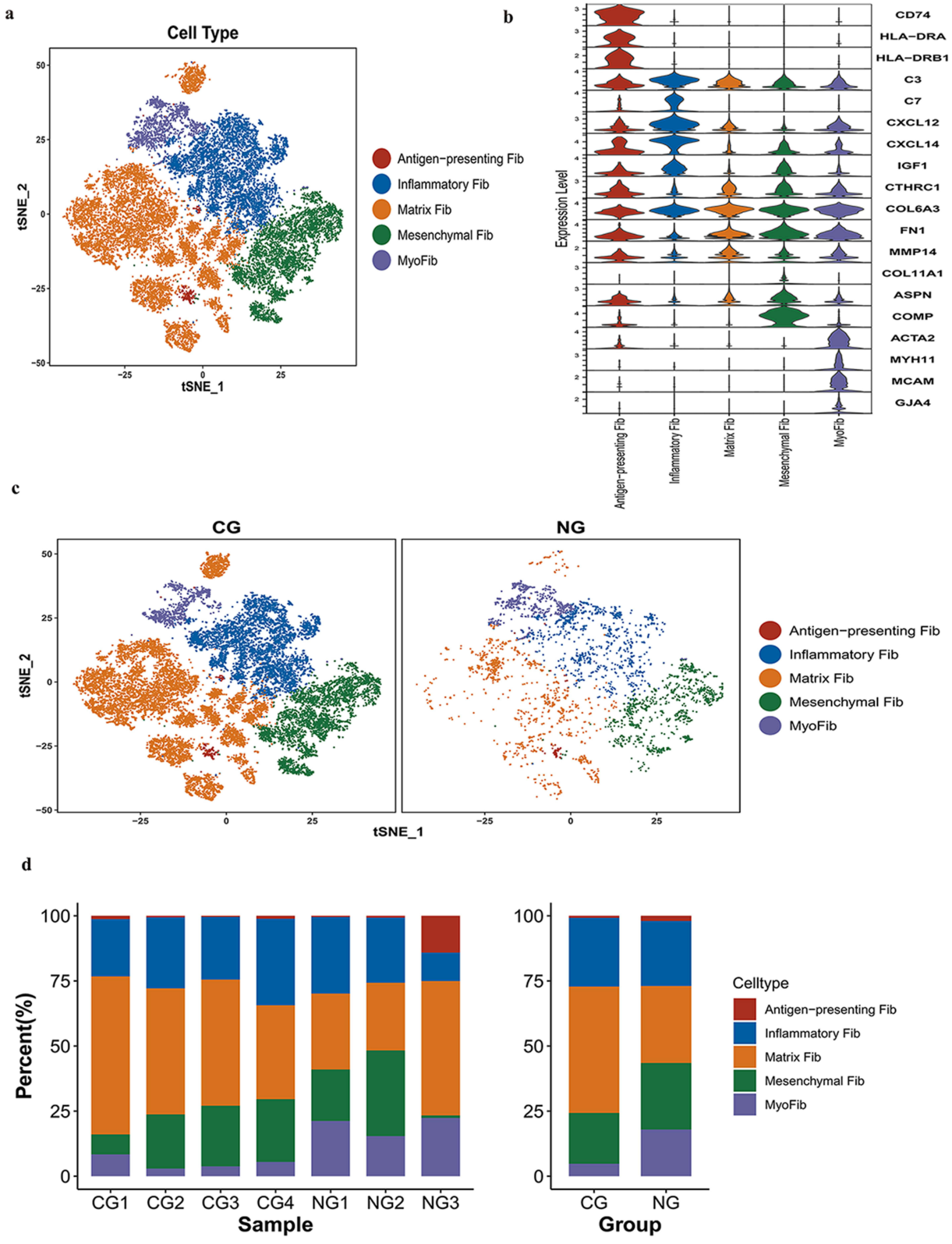

Figure 3 Clustering and classification of the fibroblasts (Fib) subclusters of deep fascia tissue (**a**). tSNE visualization of fibroblasts subclusters from deep fascia tissue. (**b**). Violin plots showing marker genes across fibroblasts subclusters. (**c**). tSNE visualization of fibroblasts subclusters from deep fascia tissue in NG and CG. (**d**). Bar plots showing the relative percentage of fibroblasts subclusters for each sample as well as in two groups (NG and CG).

Abbreviations: NG, necrotizing fasciitis group; CG, control group.

https://doi.org/10.2147/JIR.S496650

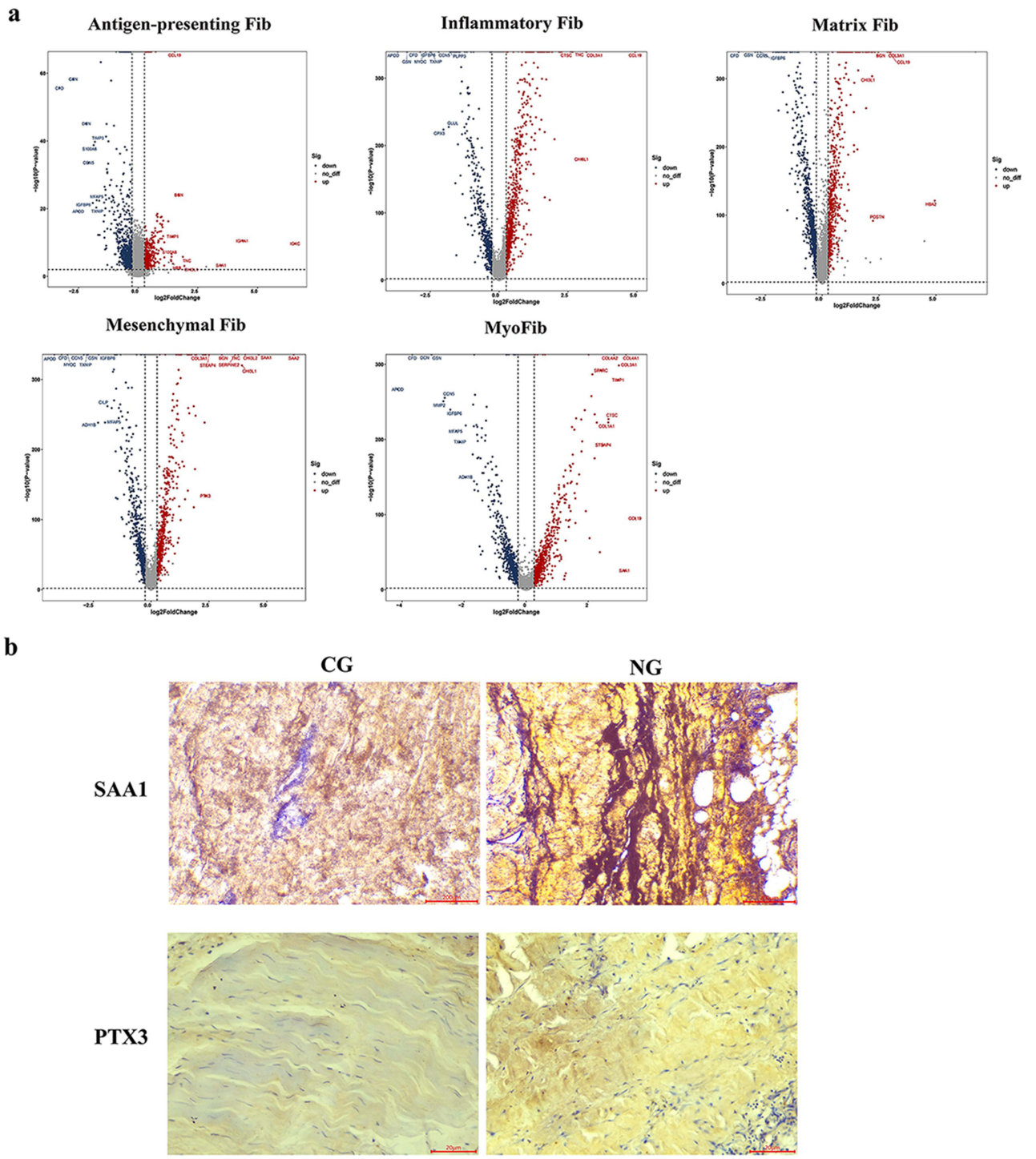

Figure 4 Comparison of differentially expressed genes (DEGs) of fibroblasts (Fib) subclusters in two groups (NG and CG) and partial DEGs were verified. (**a**). Comparison of Top 10 DEGs in two groups (NG and CG); (**b**). SAA1 and PTX3 were verified by immunohistochemistry staining.
Abbreviations: NG, necrotizing fasciitis group; CG, control group.

partook "immune response", "neutrophil chemotaxis", "lymphocyte chemotaxis" and "response to tumor necrosis factor" (Supplementary Figure 1). KEGG pathway indicated that the PI3K-Akt, NF-kappa B, and HIF-1 signaling pathway may get involved in regulating NF (Supplementary Figure 2).

Macrophage Subsets in the Two Groups

We identified five subclusters: SPP1^{+}Mac0, IL1B^{+} Mac1, C1QA^{+} Mac2, SPP1^{+}M2 and IFN-act Mac2[20,21] (Figure 5a-c). We observed higher proportions of SPP1^{+} Mac0, IL1B^{+} Mac1, and SPP1^{+}M2, as well as lower proportions of C1QA^{+} Mac2 and IFN-act Mac2 in the NG (Figure 5d and Table 2).

Next, we compared the top 10 DEGs of higher proportions of Mac in the two groups. Notably, *TIMP1, MARCO, VCAN, STAB1*,and *APOC1* were up-regulated in SPP1^{+} Mac0 (Figure 6a). The GO term indicated that this subpopulation was engaged into "positive regulation of cell population proliferation", and "signal transduction" (Supplementary Figure 3). KEGG pathway implied that the bacterial invasion of epithelial cells, and HIF-1 signaling pathway may be involved in regulating NF (Supplementary Figure 4). In addition, S100 family (*S100A9, S100A8, S100A12), IFITM2*, and *FCGR3B* were up-regulated in IL1B^{+} Mac1 (Figure 6a). The GO term indicated that this subpopulation was engaged into in "positive regulation of inflammatory response", "neutrophil chemotaxis", "immune system process" and "defense response to bacterium" (Supplementary Figure 3). KEGG pathway implied that the PI3K-Akt, IL-17, and Jak-STAT signaling pathway, as well as Cytokine–cytokine receptor interaction, Fc gamma R-mediated phagocytosis, and Staphylococcus aureus infection may be involved in regulating NF (Supplementary Figure 4). Furthermore, *PPIB, VACN, HSPA5, MARCO, S100A8, MT1G* were up-regulated in SPP1^{+}M2 (Figure 6a). Then, we used IHC staining to verify the expression of STAB1, MARCO, S100A9, S100A8, and S100A12 in two groups (Figure 6b). The GO term indicated that this subpopulation was engaged into "neutrophil chemotaxis", "immune system process", and "acute inflammatory response" (Supplementary Fig.3). KEGG pathway implied that bacterial invasion of epithelial cells, the HIF-1, IL-17, and PPAR signaling pathway may be engaged into regulating NF (Supplementary Figure 4).

T-Cell Subsets in the Two Groups

We subgrouped T cells into six cell subtypes: Cytotoxic CD8 T, GZMK^{+} effector CD4 T-cell (Teff), GZMK^{+} CD8 Teff, nature killer cells (NK), NKT, and innate lymphoid cell-3 subtypes (Figure 7a-c).[20] We observed higher proportions of GZMK^{+} CD4 Teff, as well as lower proportions of Cytotoxic CD8 T, and NKT in NG (Figure 7d and Table 2). Notably, *RPS26, IGHA1*, and *RPL7* were up-regulated in GZMK^{+} CD4 Teff (Figure 8). The GO term indicated that this subpopulation was engaged into "defense response to bacterium", and "immune response" (Supplementary Figure 5). KEGG pathway implied that the bacterial invasion of epithelial cells, IL-17, and Rap1 signaling pathway may be engaged into regulating NF (Supplementary Figure 6).

Cell–Cell Crosstalk

CellPhoneDB was used to assess the interactions among Fib, Mac and T-cell subclusters that had higher proportions in response to NF (Figure 9a and b). Antigen-presenting Fib and GZMK^{+} CD4 Teff mainly interacted with other subsets via the CD74-MIF, CD74-COPA and CD74-APP (Figure 9c). IL1B^{+} Mac1 were more likely to use CD74-MIF, CD74-COPA, CD74-APP, C5AR1-RPS19 and TYROBP-CD44 (Figure 9c), while SPP1^{+} Mac0 and SPP1^{+}M2, mainly interacted with other subsets via the TYROBP-CD44, LGALS9-CD44, SPP1-CD44, C5AR1-RPS19, CD74-MIF, CD74-COPA and CD74-APP (Figure 9c). Additionally, mesenchymal Fib mainly interacted with other subsets via the ANXA-FPR axis, NR3C1-CXCL8, CD44-HBEGF, LGALS3-MERTK, and BSG-PPIA, whereas myoFib mainly interacted with other subsets via the HGF-CD44, CD44-HBEGF, NR3C1-CXCL8, LGALS3-MERTK, and BSG-PPIA.

Discussion

NF, a severe infectious disease, may cause a series of serious complications, such as muscle necrosis, amputation, or even death.[2,22] Given the challenges of early diagnosis and effective treatment, potential mechanisms of NF are urgently investigated. Deep fascia has been regarded as the fiber tissue surrounding muscles[23] and previous studies focused on healing and repair mechanisms.[24–26] Our recent study has demonstrated the immunologic function of deep fascia, which has been previously neglected, under high pressure in the compartment.[23] As we know, we are the first to focus on fascia from NF patients using scRNA-seq. Here, we found the significant variations of fibroblast subtypes and macrophage

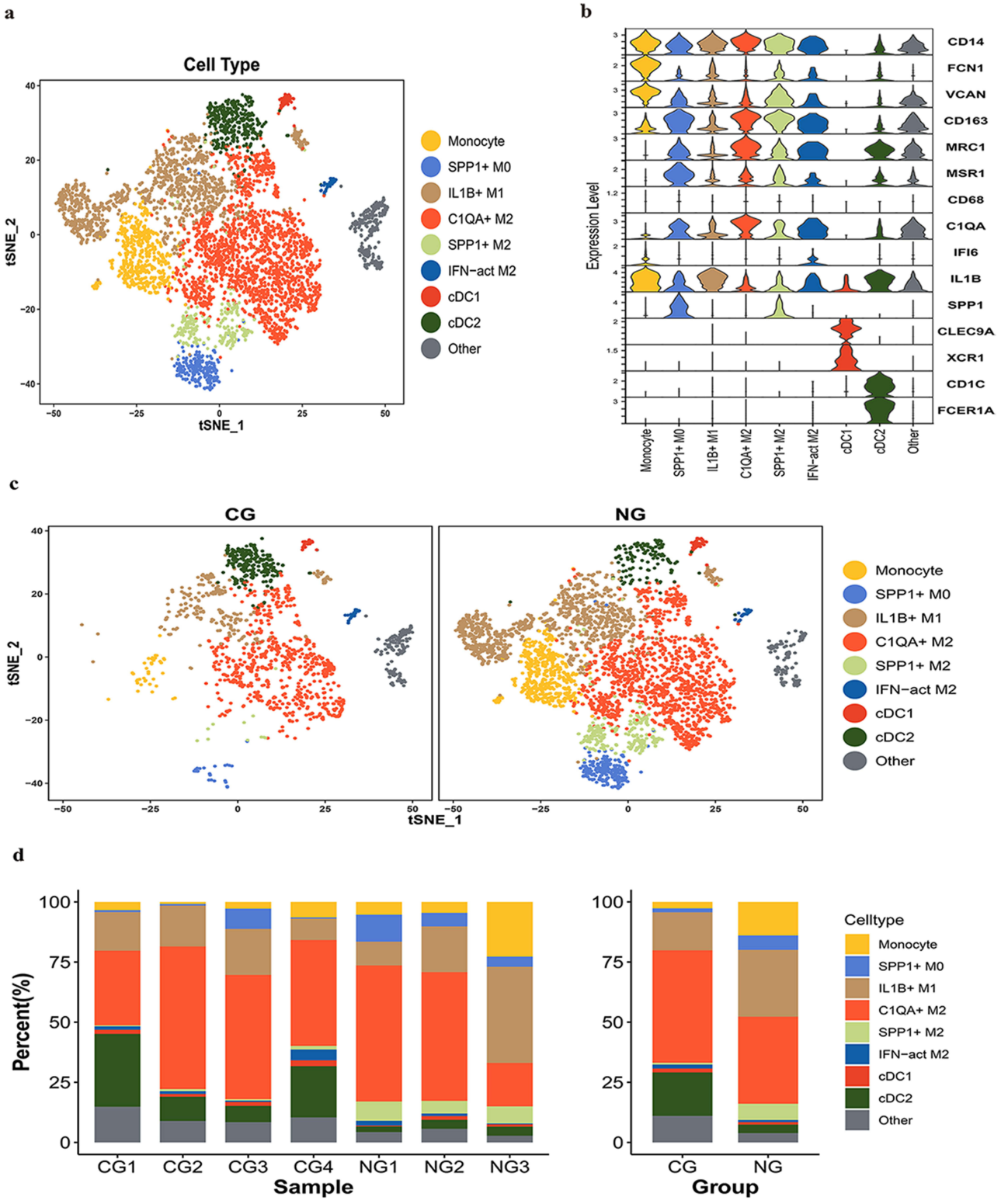

Figure 5 Clustering and classification of myeloid cell subclusters of deep fascia tissue (**a**). tSNE visualization of myeloid cell subclusters from deep fascia tissue. (**b**). Violin plots showing marker genes across myeloid cell subclusters. (**c**). tSNE visualization of myeloid cell subclusters from deep fascia tissue in NG and CG. (**d**). Bar plots showing the relative percentage of myeloid cell subclusters for each sample as well as in two groups (NG and CG).
Abbreviations: NG, necrotizing fasciitis group; CG, control group.

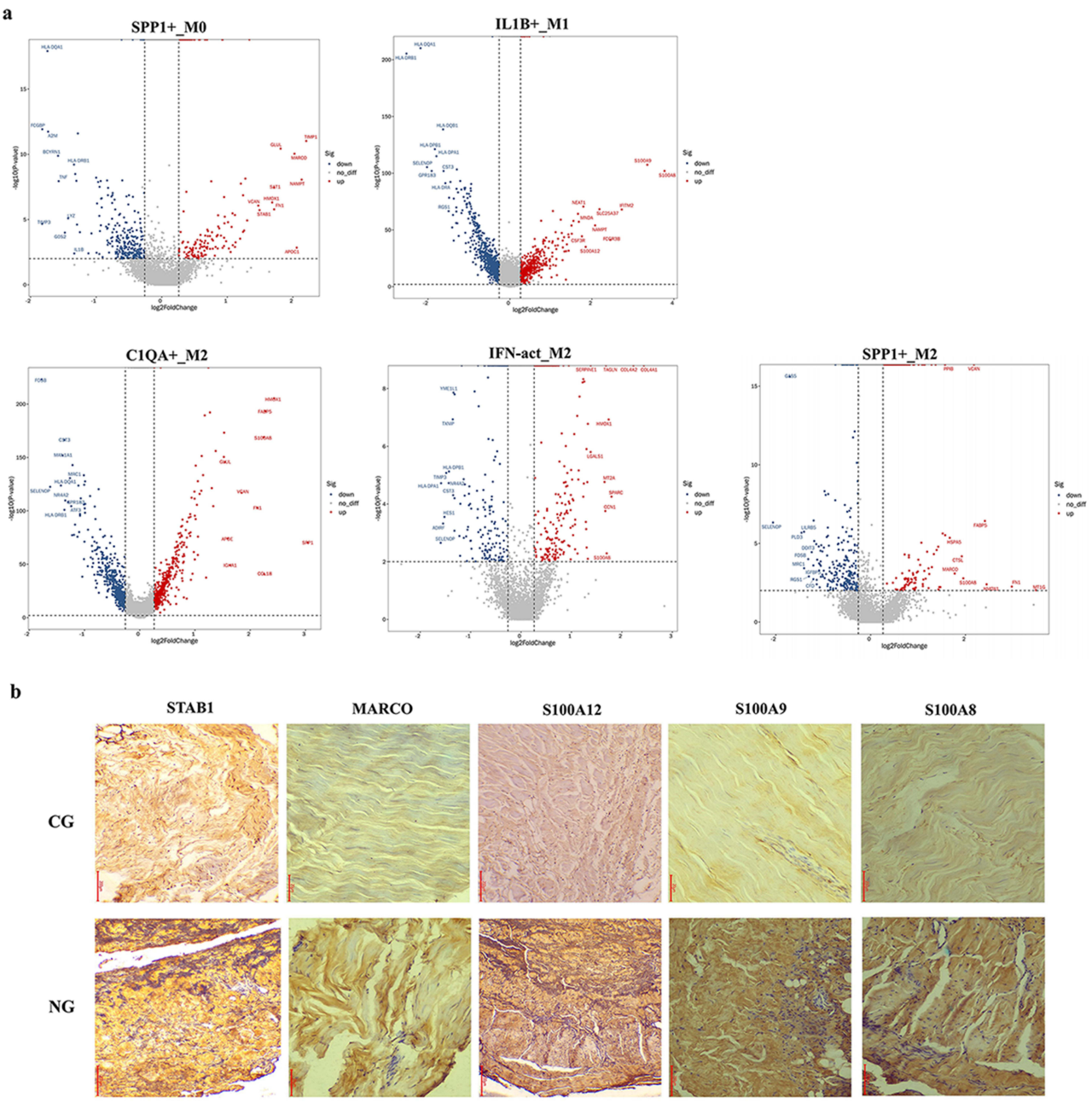

Figure 6 Comparison of differentially expressed genes (DEGs) of macrophage (Mac) subclusters in two groups (NG and CG) and partial DEGs were verified. (**a**). Comparison of Top 10 DEGs in two groups (NG and CG); (**b**). STAB1, MARCO, S100A8, S100A9, and S100A12 were verified by immunohistochemistry staining.
Abbreviations: NG, necrotizing fasciitis group; CG, control group.

subclusters derived from deep fascia, as well as the DEGs, implying the immunologic function of deep fascia in response to NF.

Fibroblast, a main cell type of deep fascia, is highly heterogeneous in distinct organs,[27,28] which has been reported in various fibrotic diseases, such as lung fibrosis, and keloid.[29–31] Our latest research found five fibroblast subclusters with high expression of fibrillar collagen genes under high pressure within the compartment. We found dramatically decreased proportions of fibroblast of deep fascia in response to infection, but we found the percentage of three subtypes increased, including antigen-presenting Fib, mesenchymal Fib, and myoFib. As we know, SAA1, one type of serum amyloid A family apolipoprotein, contributes to the regulation of inflammation and immunity in response to infectious diseases.[32–34] Lv [32] found exosomal SAA1 to be a crucial factor in regulating sepsis-induced lung injury.

https://doi.org/10.2147/JIR.S496650

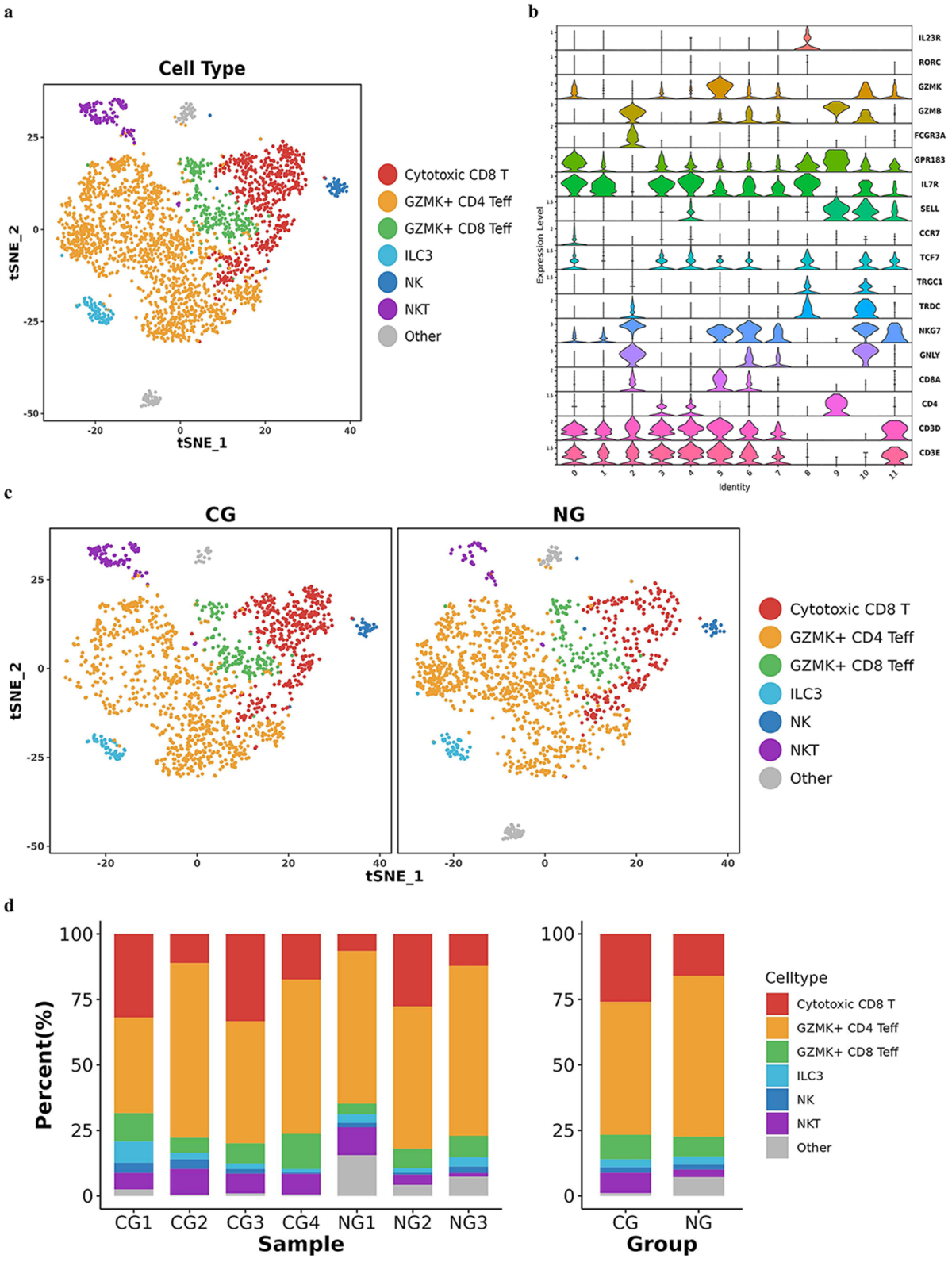

Figure 7 Clustering and classification of T cell subclusters of deep fascia tissue (**a**). tSNE visualization of T cell subclusters from deep fascia tissue. (**b**). Violin plots showing marker genes across T cell subclusters. (**c**). tSNE visualization of T cell subclusters from deep fascia tissue in NG and CG. (**d**). Bar plots showing the relative percentage of T cell subclusters for each sample as well as in two groups (NG and CG).
Abbreviation: NG, necrotizing fasciitis group; CG, control group.

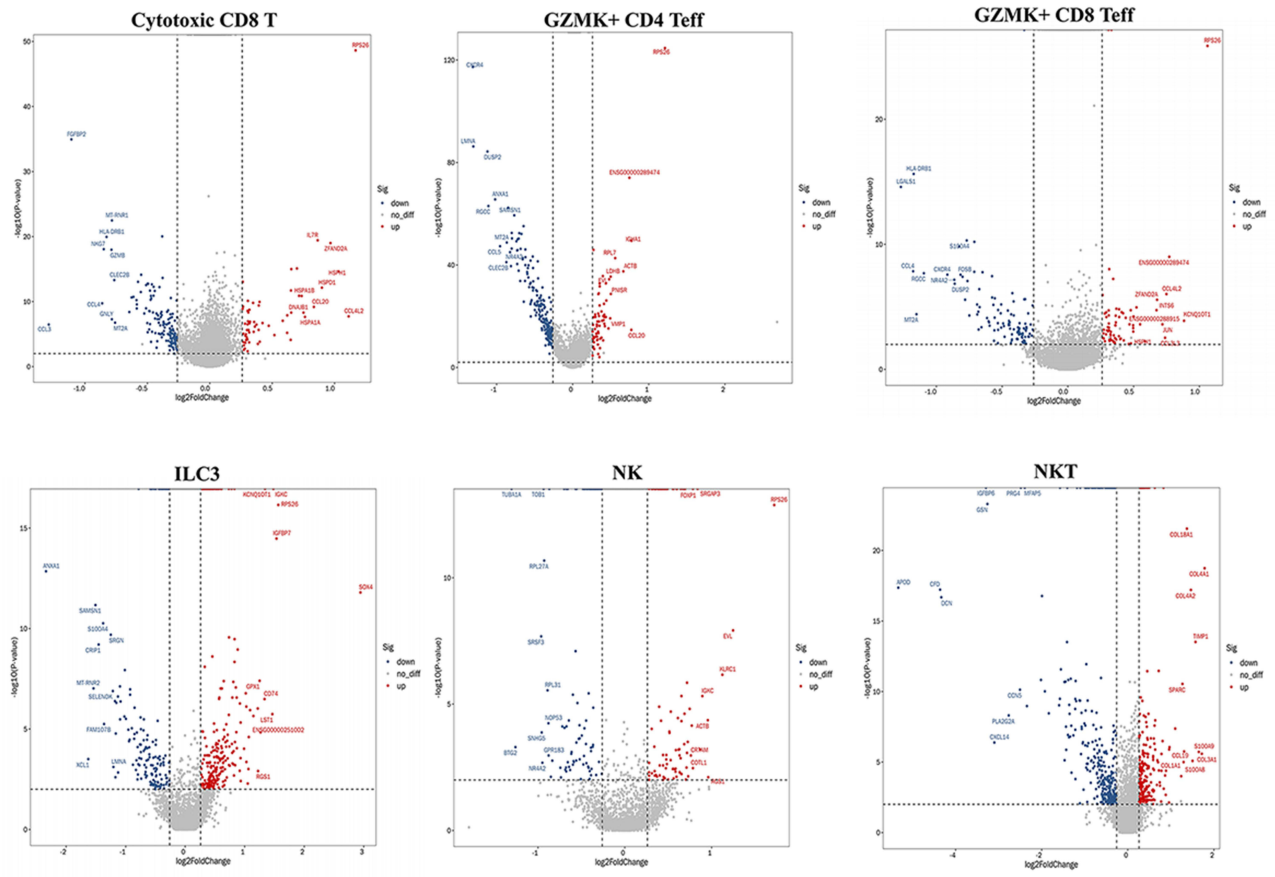

Figure 8 Comparison of differentially expressed genes (DEGs) of T cell subclusters in two groups (NG and CG).
Abbreviations: NG, necrotizing fasciitis group; CG, control group.

Additionally, SAA1 also was a biomarker in the diagnosis of sepsis.[33,34] However, the role of SAA1 among fibroblast subtypes in NF has not been elucidated. Regarding the three increased fibroblast subclusters, the level of *SAA1* was up-regulated in NG compared with CG, implying that these three subclusters were important regulators of inflammation and immunity in response to NF.

In terms of antigen-presenting Fib, it was mainly responsible for the humoral immunity against the bacteria that results in NF because it highly expressed *IGHA1* and *IGKC*, which were the major class of antibodies associated with mucosal immunity.[35] Expression of *PTX3* was higher in mesenchymal Fib under the infectious microenvironment. PTX3, which was synthesized by mononuclear phagocytes and endothelial cells at the inflammatory site,[36] is highly expressed in mice during inflammation and[37] in human response to septic shock.[38] It also was related to the severity of the condition and survival rate.[39,40] PTX3 can be a biomarker or even a candidate therapy for NF,[41] implying that mesenchymal Fib may play a determinant role in the prognostic outcome of NF. MyoFib highly expressed *SPARC* and fibrillar collagen genes, including *COL1A1, COL3A1, COL4A2*, and *COL4A1*, which mainly contributed to the structural integrity of extracellular matrix, tissues, and organs,[42,43] indicating that this subpopulation was associated with tissue repair and fibrosis of deep fascia during the development of NF. Taken together, these three increased subclusters have distinct functions in response to NF. Additionally, SAA1 and PTX3 may be biomarkers of NF to help us estimate the severity of the condition and survival rate or even as therapeutic targets.

Macrophages, which are primary innate immune cells, contributed to the maintenance of tissue homeostasis. Macrophages are divided into two major subclusters: M1 macrophages contribute to a pro-inflammatory role leading to antimicrobial activity, while M2 macrophages play an anti-inflammatory role in promoting tissue repair.[44] Therefore, the ratio of M1/M2 may be a key factor to determine the prognostic outcome or even a therapeutic target in some

https://doi.org/10.2147/JIR.S496650

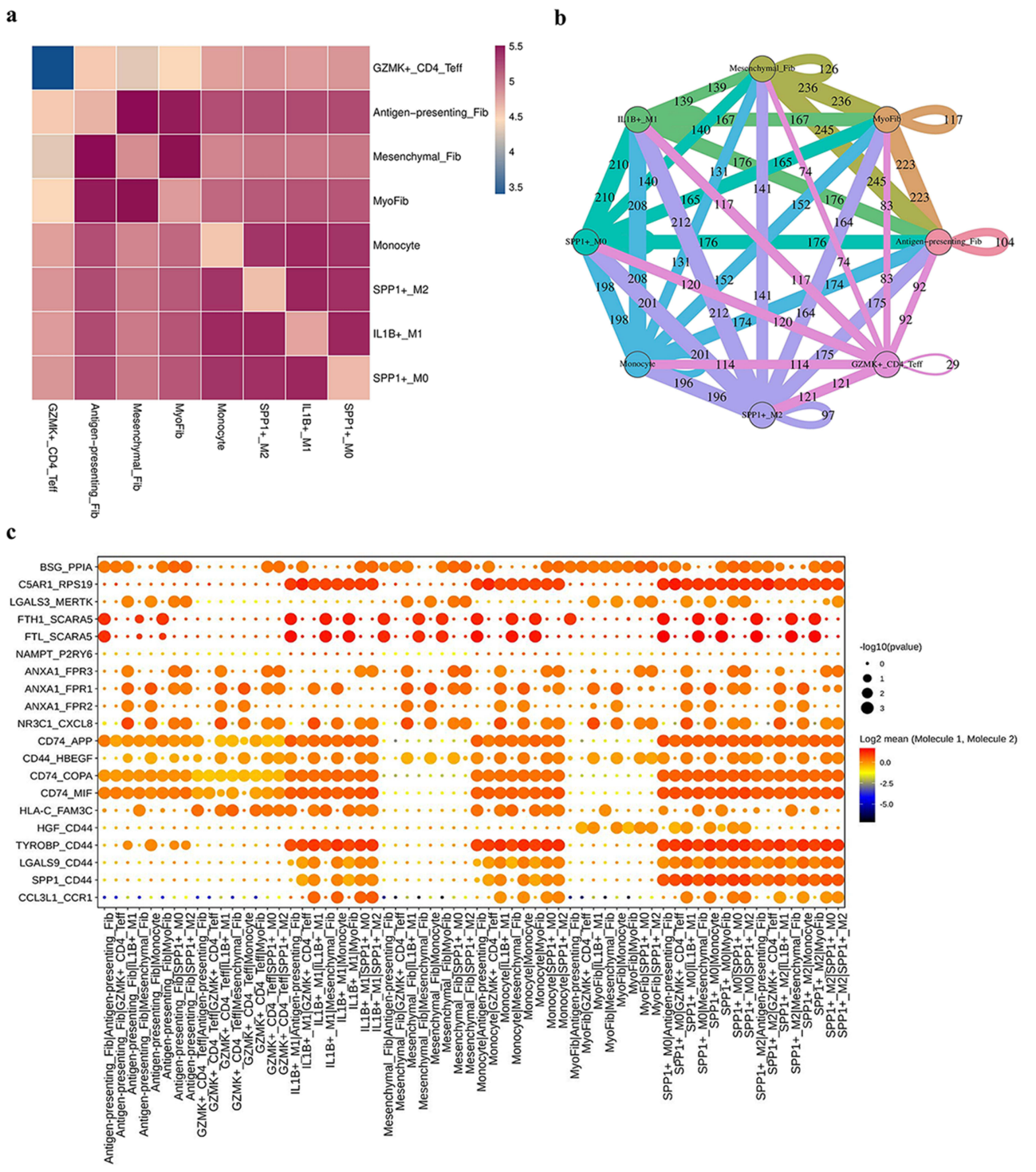

Figure 9 Crosstalk among T cell, fibroblasts and myeloid cell subclusters. (**a**). Heatmap presents the key cellular interaction among T cell, fibroblasts and myeloid cell subclusters; (**b**). Network diagram shows interaction among T cell, fibroblasts and myeloid cell subclusters; (**c**). Dot plot shows the significant ligand-receptor pairs among T cell, fibroblasts and myeloid cell subclusters.

Abbreviations: NG, necrotizing fasciitis group; CG, control group.

diseases, such as infectious disease. In the current study, we found SPP1^{+} Mac0, IL1B^{+} Mac1, and SPP1^{+}M2 with increased proportions during the process of NF. It is well known that M1 is predominant to anti-infection during the development of NF by pro-inflammatory activity and M2 is mainly related to tissue repair and anti-inflammatory.

In our study, the levels of S100 family contribute to immune response to infections, were up-regulated in IL1B$^+$ Mac1. Evidence indicated that they were related to disease pathogenesis.[45–47] S100 proteins can act as chemoattracts to the co-ordinate migration and chemotaxis of immune cells to infection sites.[45] For example, S100A8/A9 have been demonstrated to recruit monocytes and neutrophils and their pro-inflammatory functions can be activated under pathological conditions.[48–50] Additionally, S100A12 can produce IL-6 and IL-8,[51] and also contributes to fighting infections.[52] Ongoing studies have shown that S100A8, S100A9 and S100A12 can be orchestrated by bacterial infection, and they can take part in pathogen killing as antimicrobial effectors or as damage-associated molecular pattern molecules.[46,47] These findings implied the crucial role of IL1B$^+$ Mac1 in anti-infection by up-regulating the expression of *S100A8, S100A9*, and *S100A12*, which can be biomarkers or even potential therapeutic strategies. Interestingly, we found both SPP1$^+$ Mac0 and SPP1$^+$M2 with high expression of *MARCO* that was up-regulated on macrophages after bacterial infection and contributed to the removal of pathogens,[53] implying the important roles of SPP1$^+$Mac0 and SPP1$^+$M2 in the elimination of pathogens in response to NF. Additionally, we found that SPP1$^+$Mac0 highly expressed *STAB1* that was induced during chronic inflammation to degrade nonself and "unwanted-self" molecules and particles, indicating that SPP1$^+$Mac0 may greatly contribute to the clearance of necrotic tissue. Taken together, the balance of M1/M2 is the key therapeutic target for NF intervention. Furthermore, S100 proteins and MARCO may be biomarkers of NF to help clinicians assess the severity of the condition and survival rate, or even as potential therapeutic strategies.

Monocytes can mediate host antimicrobial defense and differentiate into macrophages.[54,55] In our study, we found an increased proportion of monocytes with an anti-infection role in response to NF by highly expressing pro-inflammatory (*IL1*) and chemokine (*CCL4L2* and *CCL4*) genes that contributed to the recruitment of macrophages and differentiation towards M1. However, regrettably, we failed to sort out the monocyte subclusters based on the published articles. The anti-infection role of monocytes/macrophage lineages may determine outcomes and can be a basis for prospective remedial management. Additionally, GZMK$^+$ CD4 Teff, the only subcluster with a higher proportion in NG, had highly expressed *IGHA1* and *CCL20* that participated in antimicrobial activity,[56] We also used CellPhoneDB to evaluate the interactions among Fib, Mac and T-cell subclusters, which had higher proportions in response to NF. We also investigated cellular interactions among higher proportions of NG via immune-related L-R pairs and discovered these subtypes mainly interacted with others by antigen-presenting Fib, GZMK$^+$ CD4 Teff, IL1B$^+$ Mac1, SPP1$^+$ Mac0 and SPP1$^+$M2 mainly interacted with other subsets via the CD74-MIF, CD74-COPA and CD74-APP, while mesenchymal Fib and myoFib mainly interacted with other subsets via the NR3C1-CXCL8, CD44-HBEGF, LGALS3-MERTK, and BSG-PPIA.

Although we first identified the variation of cells of fascia in NF patients by the scRNA-seq, there are still some limitations. First, we mainly focused on the fibroblast and macrophage subclusters because we failed to sort out others based on biomarkers from published studies, such as B cells and monocytes. Second, because of the relatively low incidence of NF, a limited number of samples may limit dynamic observation and individual differences may impact the results. Third, the lack of widely accepted NF animal models hampers the function verification of fibroblasts and macrophage subclusters.

Conclusions

We are the first to provide landscape of cellular subclusters from fascia in NF patients by scRNA-seq. We mainly found that three fibroblast subclusters and three macrophage subclusters had increased proportions in response to NF with distinct roles. The balance of M1/M2 polarization may be the key therapeutic target to determine the outcome of NF. Additionally, the levels of some proteins, such as SAA1, PTX3, S100 proteins, MARCO, and STAB1, were up-regulated in response to this life-threatening infectious disease, which may be a biomarker or even a candidate therapy for NF. These findings showed the anti-infection role of deep fascia, which provided novel insights for the therapeutic strategies for NF.

Data Sharing Statement

The original contributions presented in the study are included in the article/supplementary material; further inquiries can be directed to the corresponding authors.

Consent for Publication

Yes.

Author Contributions

All authors made a significant contribution to the work reported, whether that is in the conception, study design, execution, acquisition of data, analysis and interpretation, or in all these areas; took part in drafting, revising or critically reviewing the article; gave final approval of the version to be published; have agreed on the journal to which the article has been submitted; and agree to be accountable for all aspects of the work.

Funding

The research was supported by The Natural Science Foundation of Hebei (H2024206134, H2024206027, H2024206022, H2023206159).

Disclosure

No competing interests reported in regard to this work.

References

1. Pakula C-H, Chang H-C, Pasupathy S, et al. Necrotizing fasciitis: clinical presentation, microbiology, and determinants of mortality. *J Bone Joint SurgAm*. 2003;85-A:1454–1460. doi:10.1177/000313481207801010
2. Stevens DL, Bryant AE. Necrotizing soft-tissue infections. *N Eng J Med*. 2017;377(23):2253–2265. doi:10.1056/NEJMra1600673
3. van Stigt SFL, de Vries J, Bijker JB, et al. Review of 58 patients with necrotizing fasciitis in The Netherlands. *World J Emerg Surg*. 2016;11(1):21. doi:10.1186/s13017-016-0080-7
4. Sarani B, Strong M, Pascual J, Schwab CW. Necrotizing fasciitis: current concepts and review of the literature. *J Am Coll Surg*. 2009;208 (2):279–288. doi:10.1016/j.jamcollsurg.2008.10.032
5. Liu SYW, Ng SSM, Lee JFY. Multi-limb necrotizing fasciitis in a patient with rectal cancer. *World J Gastroenterol*. 2006;12(32):5256–5258. doi:10.3748/wjg.v12.i32.5256
6. Tsai YH, Shen SH, Yang TY, Chen PH, Huang KC, Lee MS. Monomicrobial necrotizing fasciitis caused by Aeromonas hydrophila and Klebsiella pneumoniae. *Med Princ Pract*. 2015;24(5):416e23. doi:10.1159/000431094
7. Cheng N-C, Tai H-C, Chang S-C, Chang C-H, Lai H-S. Necrotizing fasciitis in patients with diabetes mellitus: clinical characteristics and risk factors for mortality. *BMC Infect Dis*. 2015;15(1):417. doi:10.1186/s12879-015-1144-0
8. Giuliano A, Lewis F, Hadley K, Blaisdell FW. Bacteriology of necrotizing fasciitis. *Am J Surg*. 1977;134(1):52e7. doi:10.1016/0002-9610(77) 90283-5
9. Tsai YH, Huang KC, Shen SH, Hsu WH, Peng KT, Huang TJ. Microbiology and surgical indicators of necrotizing fasciitis in a tertiary hospital of southwest Taiwan. *Int J Infect Dis*. 2012; 16:e159e65.
10. Liu Y-M, Chi C-Y, Ho M-W, et al. Microbiology and factors affecting mortality in necrotizing fasciitis. *J Microbiol Immunol Infect*. 2005;38:430e5.
11. Pakula AM, Kapadia R, Freeman B, et al. A 3-year experience with necrotizing fasciitis: favorable outcomes despite operative delays in a busy acute care hospital. *Am Surg*. 2012;78(10):1059–1062.
12. Gelbard RB, Ferrada P, Yeh DD, et al. Optimal timing of initial debridement for necrotizing soft tissue infection: a practice management guideline from the Eastern association for the surgery of Trauma. *J Trauma Acute Care Surg*. 2018;85(1):208–214. doi:10.1097/TA.0000000000001857
13. Okoye O, Talving P, Lam L, et al. Timing of redébridement after initial source control impacts survival in necrotizing soft tissue infection. *Am Surg*. 2013;79(10):1081–1085. doi:10.1177/000313481307901025
14. Boyer A, Vargas F, Coste F, et al. Influence of surgical treatment timing on mortality from necrotizing soft tissue infections requiring intensive care management. *Intensive Care Med*. 2009;35(5):847–853. doi:10.1007/s00134-008-1373-4
15. Misiakos EP, Bagias G, Patapis P, et al. Current concepts in the management of necrotizing fasciitis. *Front Surg*. 2014;1(36). doi:10.3389/ fsurg.2014.00036
16. Wong CH, Khin LW, Heng KS, Tan KC, Low CO. The LRINEC (Laboratory Risk Indicator for Necrotizing Fasciitis) score: a tool for distinguishing necrotizing fasciitis from other soft tissue infections. *Crit Care Med*. 2004;32(7):1535–1541. doi:10.1097/01. CCM.0000129486.35458.7D
17. Zhu L, Olsen RJ, Beres SB, et al. Gene fitness landscape of group A streptococcus during necrotizing myositis. *J Clin Invest*. 2019;129(2):887–901. doi:10.1172/JCI124994
18. Thänert R, Itzek A, Hoßmann J, et al. Molecular profiling of tissue biopsies reveals unique signatures associated with streptococcal necrotizing soft tissue infections. *Nat Commun*. 2019;10(1):3846. doi:10.1038/s41467-019-11722-8
19. Zhang M, Yang H, Wan L, et al. Single-cell transcriptomic architecture and intercellular crosstalk of human intrahepatic cholangiocarcinoma. *J Hepatol*. 2020;73(5):1118–1130. doi:10.1016/j.jhep.2020.05.039
20. Wu X, Liu Y, Jin S, et al. Single-cell sequencing of immune cells from anticitrullinated peptide antibody positive and negative rheumatoid arthritis. *Nat Commun*. 2021;12(1):4977. doi:10.1038/s41467-021-25246-7
21. Zhang F, Wei K, Slowikowski K, et al. Defining inflammatory cell states in rheumatoid arthritis joint synovial tissues by integrating single-cell transcriptomics and mass cytometry. *Nat Immunol*. 2019;20(7):928–942. doi:10.1038/s41590-019-0378-1

22. Nelson GE, Pondo T, Toews K-A, et al. Epidemiology of invasive group A streptococcal infections in the United States, 2005-2012. *Clin Infect Dis*. 2016;63(4):478–486. doi:10.1093/cid/ciw248
23. Wang T, Long Y, Ma L, et al. Single-cell RNA-seq reveals cellular heterogeneity from deep fascia in patients with acute compartment syndrome. *Front Immunol*. 2023;13:1062479. doi:10.3389/fimmu.2022.1062479
24. van der Wal J. The architecture of the connective tissue in the musculoskeletal system-an often overlooked functional parameter as to proprioception in the locomotor apparatus. *Int J Ther Massage Bodywork*. 2009;2:9–23. doi:10.3822/ijtmb.v2i4.62
25. Hoheisel U, Rosner J, Mense S, et al. Innervation changes induced by inflammation of the rat thoracolumbar fascia. *Neuroscience*. 2015;300:351–359. doi:10.1016/j.neuroscience.2015.05.034
26. Schleip R, Gabbiani G, Wilke J, et al. Fascia is able to actively contract and may thereby influence musculoskeletal dynamics: a histochemical and mechanographic investigation. *Front Physiol*. 2019;10:336. doi:10.3389/fphys.2019.00336
27. Tracy LE, Minasian RA, Caterson EJ. Extracellular matrix and dermal fibroblast function in the healing wound. *Adv Wound Care*. 2016;5 (3):119–136. doi:10.1089/wound.2014.0561
28. Travers JG, Kamal FA, Robbins J, et al. Blaxall: cardiac fibrosis: the fibroblast awakens. *Circ Res*. 2016;118(6):1021–1040. doi:10.1161/CIRCRESAHA.115.306565
29. Layton TB, Williams L, McCann F, et al. Cellular census of human fibrosis defines functionally distinct stromal cell types and states. *Nat Commun*. 2020;11:2768. doi:10.1038/s41467-020-16264-y
30. Valenzi E, Bulik M, Tabib T, Morse C, Sembrat J, Trejo Bittar H. Single-cell analysis reveals fibroblast heterogeneity and myofibroblasts in systemic sclerosis-associated interstitial lung disease. *Ann Rheumatol Dis*. 2019;78(10):1379–1387. doi:10.1136/annrheumdis-2018-214865
31. Adams TS, Schupp JC, Poli S, Ayaub EA, Neumark N, Ahangari F. Single-cell RNA-seq reveals ectopic and aberrant lung-resident cell populations in idiopathic pulmonary fibrosis. *Sci Adv*. 2020;6:eaba1983. doi:10.1126/sciadv.aba1983
32. Lv Z, Duan S, Zhou M, et al. Mouse bone marrow mesenchymal stem cells inhibit sepsis-induced lung injury in mice via exosomal SAA1. *Mol Pharm*. 2022;19(11):4254–4263. Epub 2022 Sep 29. PMID: 36173129. doi:10.1021/acs.molpharmaceut.2c00542
33. Sui YD, Xin WN, Feng LL. Comparison of the clinical application values of PCT, hs-CRP and SAA detection in the early diagnosis of sepsis. *Pak J Med Sci*. 2020;36(7):1683–1687. PMID: 33235597; PMCID: PMC7674894. doi:10.12669/pjms.36.7.2544
34. Balayan S, Chauhan N, Chandra R, Jain U. Molecular imprinting based electrochemical biosensor for identification of serum amyloid A (SAA), a neonatal sepsis biomarker. *Int J Biol Macromol*. 2022;195:589–597. Epub 2021 Dec 14. PMID: 34920065. doi:10.1016/j.ijbiomac.2021.12.045
35. Kunhareang S, Zhou H, Hickford JG. Novel sequence of the porcine IGHA gene. *Mol Immunol*. 2009;47(2–3):147–148. Epub 2009 Sep 24. PMID: 19781787. doi:10.1016/j.molimm.2009.08.029
36. Vouret-Craviari V, Matteucci C, Peri G, et al. Expression of a long pentraxin, PTX3, by monocytes exposed to the mycobacterial cell wall component lipoarabinomannan. *Infect Immun*. 1997;65(4):1345–1350. PMID: 9119472; PMCID: PMC175138. doi:10.1128/iai.65.4.1345-1350.1997
37. Polentarutti N, Bottazzi B, Di Santo E, et al. Inducible expression of the long pentraxin PTX3 in the central nervous system. *J Neuroimmunol*. 2000;106(1–2):87–94. doi:10.1016/S0165-5728(00)00214-9
38. Muller B, Peri G, Doni A, et al. Circulating levels of the long pentraxin PTX3 correlate with severity of infection in critically ill patients. *Crit Care Med*. 2001;29(7):1404–1407. doi:10.1097/00003246-200107000-00017
39. Dias AA, Goodman AR, Dos Santos JL, et al. TSG-14 transgenic mice have improved survival to endotoxemia and to CLP-induced sepsis. *J Leukoc Biol*. 2001;69(6):928–936. doi:10.1189/jlb.69.6.928
40. Porte R, Davoudian S, Asgari F, et al. The long pentraxin PTX3 as a humoral innate immunity functional player and biomarker of infections and sepsis. *Front Immunol*. 2019;10:794. PMID: 31031772; PMCID: PMC6473065. doi:10.3389/fimmu.2019.00794
41. Bottazzi B, Inforzato A, Messa M, et al. The pentraxins PTX3 and SAP in innate immunity, regulation of inflammation and tissue remodelling. *J Hepatol*. 2016;64(6):1416–1427. Epub 2016 Feb 26. PMID: 26921689; PMCID: PMC5414834. doi:10.1016/j.jhep.2016.02.029
42. Gelse K, Poschl E, Aigner T, et al. Collagens: structure, function, and biosynthesis. *Adv Drug Deliv Rev*. 2003;55(12):1531–1546. doi:10.1016/j.addr.2003.08.002
43. Peterszegi G, Andrès E, Molinari J, Ravelojaona V, Robert L. Effect of cellular aging on collagen biosynthesis: i. methodological considerations and pharmacological applications. *Arch Gerontol Geriatr*. 2008;47(3):356–367. doi:10.1016/j.archger.2007.08.019
44. Nahrendorf M, Swirski FK. Abandoning M1/M2 for a network model of macrophage function. *Circ Res*. 2016;119(3):414–417. doi:10.1161/CIRCRESAHA.116.309194
45. Zhang C, Zhang Q, Wang J, et al. Transcriptomic responses of S100 family to bacterial and viral infection in zebrafish. *Fish Shellfish Immunol*. 2019;94:685–696. Epub 2019 Sep 20. PMID: 31546038. doi:10.1016/j.fsi.2019.09.051
46. Zackular JP, Chazin WJ, Skaar EP. Nutritional immunity: S100 proteins at the host-pathogen interface. *J Biol Chem*. 2015;290(31):18991–18998. doi:10.1074/jbc.R115.645085
47. Gross SR, Sin CG, Barraclough R, Rudland PS. Joining S100 proteins and migration: for better or for worse, in sickness and in health, Cell. *Mol Life Sci*. 2014;71(9):1551–1579.
48. Eue I, Pietz B, Storck J, et al. Transendothelial migration of 27E10+ human monocytes. *Int Immunol*. 2000;12(11):1593–1604. doi:10.1093/intimm/12.11.1593
49. Nisapakultorn K, Ross KF, Herzberg MC. Calprotectin expression inhibits bacterial binding to mucosal epithelial cells. *Infect Immun*. 2001;69 (6):3692–3696. doi:10.1128/IAI.69.6.3692-3696.2001
50. Sroussi HY, Kohler GA, Agabian N, et al. Substitution of methionine 63 or 83 in S100A9 and cysteine 42 in S100A8 abrogate the antifungal activities of S100A8/A9: potential role for oxidative regulation. *FEMS Immunol Med Microbiol*. 2009;55(1):55–61. doi:10.1111/j.1574-695X.2008.00498.x
51. Yang Z, Yan WX, Cai H, et al. S100A12 provokes mast cell activation: a potential amplification pathway in asthma and innate immunity. *J Allergy Clin Immunol*. 2007;119(1):106–114. doi:10.1016/j.jaci.2006.08.021
52. Realegeno S, Kelly-Scumpia KM, Dang AT, et al. S100A12 is part of the antimicrobial network against mycobacterium leprae in human macrophages. *PLoS Pathog*. 2016;12(6):e1005705. doi:10.1371/journal.ppat.1005705
53. Elchaninov A, Lokhonina A, Vishnyakova P, et al. MARCO+ macrophage dynamics in regenerating liver after 70% liver resection in mice. *Biomedicines*. 2021;9(9):1129. PMID: 34572315; PMCID: PMC8471044. doi:10.3390/biomedicines9091129

54. Auffray C, Sieweke MH, Geissmann F. Blood monocytes: development, heterogeneity, and relationship with dendritic cells. *Annu Rev Immunol*. 2009;27(1):669–692. doi:10.1146/annurev.immunol.021908.132557
55. Serbina NV, Jia T, Hohl TM, et al. Monocyte-mediated defense against microbial pathogens. *Annu Rev Immunol*. 2008;26(1):421–452. doi:10.1146/annurev.immunol.26.021607.090326
56. Guesdon W, Auray G, Pezier T, et al. CCL20 displays antimicrobial activity against cryptosporidium parvum, but its expression is reduced during infection in the intestine of neonatal mice. *J Infect Dis*. 2015;212(8):1332–1340. PMID: 25838265. doi:10.1093/infdis/jiv206